A prototype was constructed to demonstrate the potential of the UTZ-based approach. The PC-based Map and Image Processing System (MIPS), produced by MicroImages, Inc. was selected as an example GIS. The MIPS GIS has a comprehensive complement of import/export routines for converting raster and vector overlay files into formats accessible by other GIS packages such as GRASS, ERDAS, and ARC-INFO and for importing data as well. The ideal UTZ-based database structure is general enough such that implementation on other GIS platforms and software is possible.

4 RESULTS AND DISCUSSION

The study successfully demonstrated that it is possible to create an UTZ-based urban terrain feature database architecture and to quickly construct a simplified prototype on a commercially-available GIS. The CONOP for database preparation suggests a multiple pass approach to build such a database in order to achieve a quick initial operating capability. The first pass would consist of delineating and classifying UTZs, LOCs, and nodes. These vector elements, when linked by class to physical characteristic and MOUT attribute database tables, would provide access to generic physical attribute and MOUT information useful to the commander or planner. Then, as resources and time permit, the database tables specific to each vector elements can be filled in.

A preparation rate of 8 hr / sq km was experienced, based on an average subdivision of 16.8 UTZs per km. This UTZ subdivision density is the finest mesh to be expected in practice.

The user can have effectively direct access to factor overlays used in the intelligence preparation of battlefield products. This access when used in a GIS would be accomplished through queries customized for individual users, according to individual requirements. The ability to "roll one's own" would also relieve the potential bottleneck and workload on the division-level terrain analyst team during periods of high activity.

A CELLULAR AUTOMATON MODELING FOR URBAN HEAT ISLAND MITIGATION

Ichiro Embutsu, Kenji Baba
Hitachi Research Laboratory, Hitachi, Ltd.
7-1-1, Omika, Hitachi 319-12, Japan
email : embutsu@hitachi.ncgia.ucsb.edu

Michael F. Goodchild, Richard L. Church
National Center for Geographic Information and Analysis (NCGIA),
Department of Geography, University of California at Santa Barbara
Santa Barbara, CA93106

Masanao Takeyama
Faculty of Environmental Information, Keio University,
5320 Endo, Fujisawa 252, Japan

ABSTRACT

The impact of increased air temperature due to urbanization is getting so serious as to affect a thermally-benign environment and to increase energy use for cooling. For mitigating an urban heat island problem, two mitigation plans which incorporate a district heating and cooling (DHC) plant allocation and traffic control were proposed in this study. Effects of the plans were estimated using a heat island model consisting of a cellular automaton model and physical submodels with a geographic information system (GIS) through a case study of the city of San Jose, California

INTRODUCTION

Due to the urbanization of cities, we have been faced with urban environmental problems, of which an urban heat island is one typical example. Geographic information systems (GIS) have already proven they are able to provide the necessary functions for environmental modeling through many practical applications (Goodchild, 1993).

In this study, the urban heat island problem is the focus. Mitigation of the urban heat island is expected not only to maintain a thermally-benign urban environment, but also to contribute to city-scale energy saving by decreasing electricity consumption for cooling. The main concern of this study is to investigate and estimate practical mitigation plans that take advantage of GIS techniques. To model heat transfer phenomena, which are preferably modeled empirically, a cellular automaton (CA) model and a method of acquiring transition rules of the CA model from a trained artificial neural network are introduced.

AN URBAN HEAT ISLAND PROBLEM

Phenomenon and Impact on Environment

The urban heat island is a phenomenon whereby the atmospheric ambient temperature in the urban area is augmented and becomes higher than that in neighboring rural areas. In huge metropolitan areas like New York and Tokyo, intensity of the urban heat island, or the air temperature difference between urban and rural areas, can reach up to 8 degrees Celsius in summer (Oke, 1978). This air temperature difference is a consequence of increased anthropogenic heat heat release due to urban growth, and also due to the change of the urban surface from soils to asphalt/concrete.

In low and mid latitude cities, the augmented air temperature raises the discomfort level in summer, and more energy is consumed for cooling. It is reported that the increase of energy consumption by the urban heat island accounts for 12% of the annual net energy consumption for heating and cooling, even if the reduction of the energy consumption for heating due to the augmented air temperature in winter is subtracted (Landsberg, 1981). The increased energy consumption makes the heat island worse and causes a vicious circle.

Conventional Approaches

So far, several researchers have conducted intensive studies on formulating the problem and on modeling the phenomena relevant to an urban heat island occurrence (Oke,1976&1978; Terjung,1980; Ojima,1990; Saito, 1992; etc.). One of the main concerns in this paper is to estimate a quantitative effect of the mitigation plan in a reasonable scale and with a reasonable cost for determining a feasible and practical plan. However, the existing city-scale model using the city population or other characteristics of the city is not detailed enough to prioritize areas for immediate mitigation action. Though the building-scale model is detailed and precise, it is difficult to prepare all data necessary for the calibration and the execution of the model for an entire city area.

Some mitigation plans have been proposed. It is known that a plan of changing vegetation was actually conducted in California in 1970's for mitigation (Moll, 1989). Among the contributing factors to the augmentation of the air temperature, the anthropogenic heat is considered a controllable factor as well as the green cover rate, but a mitigation plan which deals with the heat release has not been investigated. The authors propose new mitigation plans which are aimed at reducing the anthropogenic heat release.

URBAN HEAT ISLAND MODEL

Classification of Heat Transfer Phenomena

In order to model the urban heat island, contributing factors to a heat budget of the urban area need to be made clear. As a first step of a modeling procedure, heat transfer phenomena relevant to the heat budget were classified with the help of urban climatology (Landsberg, 1981). As shown in **Fig.1**, six heat transfer phenomena can be classified into two categories.

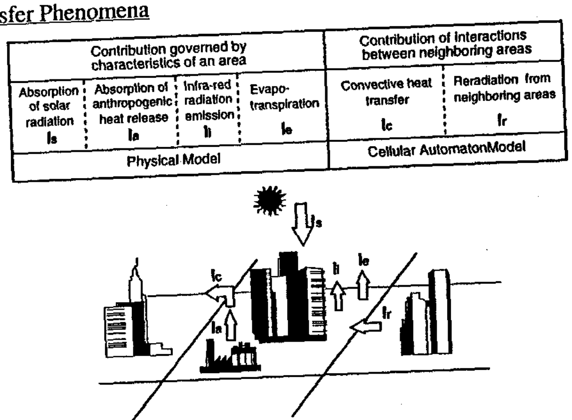

Fig.1 Phenomena of the urban heat island

The urban heat island model which is used in this study consists of submodels which describe the phenomena shown in **Fig.1**. In this model, the air temperature is explained by the summation of a background air temperature T_o and contributions of the six phenomena, as shown in **Eq.1**.

$$T = T_o + \Delta T_s + \Delta T_a + \Delta T_i + \Delta T_e + \Delta T_c + \Delta T_r \tag{1}$$

where
T : air temperature (℃), T_o : background air temperature (℃),
ΔT_s : contribution of solar radiation (℃), ΔT_a :contribution of anthropogenic heat (℃),
ΔT_i : contribution of infrared (long-wave) radiation to-and-from the air (℃),
ΔT_e : contribution of evapotranspiration (℃), ΔT_c : contribution of convection (℃),
ΔT_r : contribution of reradiation to-and-from neighboring areas (℃)

Through a review of previous studies of each phenomenon, it was found that the first group could adopt existing physical laws and models. Regarding the second group, it was obvious that the CA model could be applied. The submodels used here will be described in the following sections.

Physical Submodels

Since details of the submodels can be read in other papers, only the outline is explained here.

(1) Solar Radiation : CTTC model
A diurnal change of the solar radiation intensity has a significant influence on the air temperature variation. It is evident that the degree of its influence is not uniform for each surface type due to a difference in a thermal property. A time pattern of the air temperature rise ΔT_s in response to a change of the intensity of solar radiation can be expressed by an exponential function of time (Sharlin,1984, Swaid,1990).

To represent the thermal inertia of ground surface to the air temperature variation, CTTC (Cluster Thermal Time Constant) is used in this model. In the original CTTC model, a cluster means an area which can be assumed to have uniform thermal properties, but a cluster in this study is defined as a uniformly-partitioned cell (grid) in an area of interest. Experimental CTTC values for different surfaces such as bare soil, asphalt/concrete are available from a previous study (Swaid,1990).

(2) Anthropogenic Heat Release
Though the contribution of the anthropogenic heat is much smaller than that of the solar radiation, this heat release is important in terms of the mitigation of the urban heat island for the reason that it is a controllable factor of the heat budget in a city. The air temperature variation ΔT_a can be obtained from the specific heat of the air, assuming that the released heat in a cell diffuses uniformly in the cell space within a simulation time step.

Large sources of the anthropogenic heat in a city are power plants, incinerators, air conditioning units, vehicles, etc. If heat release from these sources could be reduced by some means, it is expected to lower the air temperature. To estimate the wasted heat, a method using average energy use and traffic flow per unit area (square meter) for each landuse type is used. The data relevant to the estimation for the San Jose area was compiled from published materials (U.S. DOE/EIA,1992; PG & E,1992; City of San Jose, 1993).

(3) Infrared Radiation : Stefan-Boltzmann law
It is known that the total energy radiated from a black body is proportional to the fourth power of the body's temperature. This law is applicable in estimating heat exchange by the infrared radiation between the surface and the air. The heat exchange depends on the building structure which changes the openness of the ground surface to the sky. To represent this openness, SVF (Sky View Factor; Oke, 1981) is calculated from a mean building height and a mean urban canyon width and incorporated into this submodel.

(4) Evapotranspiration : Penman model
Evapotranspiration is water loss through transpiration from vegetation and evaporation from wet surfaces. The latent heat for evaporating water is absorbed by the air, and this causes cooling in the air. Instead of measured data which was not available, the Penman model (Doorenbos, 1977), which has been recommended by FAO (Food and Agriculture Organization of the United Nations) for irrigation planning, is introduced. In this model, the evapotranspiration rate is explained as a function of vegetation type and humidity.

The Penman model is applicable not only to the surface covered with vegetation, but also to an open water surface such as a lake using a different crop coefficient. Also, it is applicable to bare soil surfaces, however, the latent heat for evaporating water is mainly absorbed by the soil itself, so its contribution to the air temperature is considered small. Thus, the evapotranspiration of the bare soil is neglected in this simulation.

Cellular Automaton Submodel (Convection & Reradiation)

In the cellular automaton modeling, a simulated area is partitioned into regular grid cells as shown in **Fig.2**, and phenomena which occur in this area are represented by the state value of the cells. The dynamics of the phenomena is described with a set of rules, that is so-called transition rules. The transition rules are usually written in if-then format or table format to show explicitly the interactions between a cell and its neighboring cells. Starting with a certain initial state, the values of the cells in a cellular space are updated according to the transition rules. If we could make an appropriate set of the transition rules, the cellular automaton model would allow us to simulate the phenomena occurring in a city of interest.

The convection and reradiation from neighboring areas were intended to be modeled with the cellular automata, but observational data of these two phenomena was not available. Furthermore, it was almost impossible to know the contributions of the convective heat transfer and the reradiation separately. For these reasons, these two phenomena are dealt with as a combined contribution ΔT_{inter}. The estimated value of ΔT_{inter} can be obtained from **Eq.1** using the observed and calculated values of other contributions.

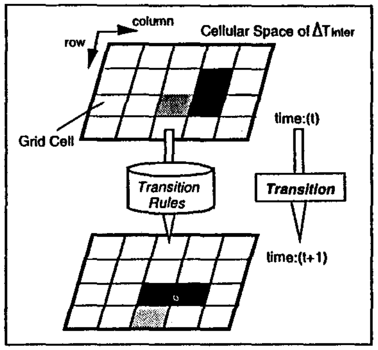

Fig.2 A cellular automaton model

The transition rules are usually created based on a priori and empirical knowledge of the phenomena of interest. For urban environmental applications, due to the complexity, it is sometimes difficult to make a set of proper transition rules. As one solution to this difficulty, a rule extraction method developed by the authors is introduced.

Transition Rule Extraction Method Using a Neural Network

The rule extraction method makes use of an artificial neural network which simulates human learning. The procedure consists of three steps of data handling. At the first step, training data which represents typical states of phenomena of interest is selected from historical data relevant to the phenomena. After this selection, a three-layered artificial neural network is trained using the selected training data. As a training algorithm, an Error Backpropagation Method (Rumelhart, 1986) is applied. By this training step, the underlying dynamics included in the training data is acquired in the network as a set of weight parameters which represent the intensities of the interconnections between neurons assigned in neighboring layers.

At the last step, the acquired dynamics in the network are converted into explicit if-then type rules with the analysis of the weight parameters. Further details of this method can be read in previous papers (Baba,1990; Embutsu,1991).

INVESTIGATION OF MITIGATION PLANS

As described earlier, a mitigation plan which facilitates the heat absorption through evapotranspiration came into actual use in some cities. But this mitigation plan was not a sweeping remedy for the problem. The authors focus on reducing the anthropogenic heat release from human activities, especially investigations from building heat and traffic.

DHC Plants Allocation

In terms of energy saving, some part of the released heat from buildings is considered to be an energy source that should be reused. If we could recover or reduce the released heat by some means, it is expected that the air temperature will fall and it will contribute to energy saving. In the field of district heating and cooling (DHC), a heat pump is widely used as a heat recovering device. As shown in **Fig.3**, the heat pump can extract heat from a cold reservoir into a hot reservoir (Kraushaar, 1993). The recovered heat is usually hot enough to be used for heating and hot water use.

Important points to lower the air temperature is to recover or reduce the heat which directly affects the air temperature and not to emit the heat to the air after using the recovered heat. The authors propose two alternatives to meet these points.

<Plan 1 : Recovering the wasted heat from buildings>
In this plan, wasted heat from a large heat source is recovered by the heat pump, and recovered heat is provided to the buildings for hot water use through the DHC lines (see **Fig.4 (a)**). Preferable heat sources for this plan are large facilities such as power plants, incinerators, etc.

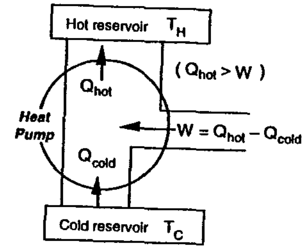

Fig. 3 A heat pump

<Plan 2 : Reducing the wasted heat from buildings>
Ordinary air conditioners exhaust the heat from their outside units (condensers) to the air, and this is one of the predominant heat sources in built-up areas. In this second plan, the air conditioners of buildings are replaced by the cooling from the DHC plant. The recovered heat within the buildings is transferred through the DHC line into the sewer line which is used as a heat sink (see **Fig.4 (b)**).

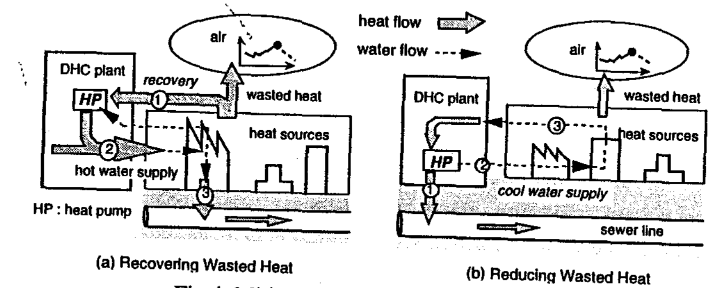

Fig.4 Mitigation plans (DHC allocation)

Traffic Control

In commercial and office areas, traffic heat is not less than the wasted heat from the buildings. Other than the improvement of an automobile fuel rate (average of American car 20.92 mile/Gallon; DOE, 1992), reducing the traffic flow in the areas suffered from the high air temperature can be a more drastic counterplan for the problem.

<Plan 3 : Reducing the waste heat from automobiles>
This plan aims at reducing the traffic flow by a traffic control . Recent research on Intelligent Vehicle Highway System (IVHS) show the possibility to control traffic flow by coordinating traffic signals in an area of interest (Khan, 1993; etc.). Though it seems difficult to reduce traffic flow in residential areas, it is considered feasible in commercial and office areas.

As alternative for reducing the waste heat from automobiles, a car pool system which prohibits single occupancy (driver only) vehicles from entering restricted areas can be a possibility. Actually, this system is applied in Singapore and is proven effective in reducing the traffic flow, though its main purpose was to mitigate traffic congestion.

DATA AND SIMULATION METHOD

Model City (City of San Jose, CA)

A case study of an urban heat island required a city that satisfied the following criteria; 1) a large population, 2) cooling and heat demand, 3) geographical and climatic characteristics that impede regional atmospheric circulation., 4) digital data. Unfortunately, no city met all of these criteria, as the fourth criterion excluded many cities from candidates. With some compromise, the city of San Jose in California was selected as a model city.

Database

Data necessary to run the urban heat island model was collected from several sources and stored in GRASS (Geographic Resource Analysis Support System), which is a raster-based GIS developed by U.S. Army Construction Engineering Research Laboratory (Shapiro, 1993). The collected data can be classified into four categories.

1) Meteorological data : air temperature, wind velocity, wind direction data measured hourly in several climatic stations were provided by BAAQMD (Bay Area Air Quality Management District) office in San Jose.
2) San Jose city data : basic data of the city of San Jose such as landuse, building height, and traffic volume was obtained from the city of San Jose (City of San Jose, 1993).
3) Energy data : energy consumption data for each landuse type, seasonal and daily demand patterns was obtained from reports publ··hed by Pacific Gas & Electric Company (PG & E, 1992). Some additional data was obtain.d from Government publications from U.S. Department of Energy (U.S. DOE/EIA, 1992).
4) Satellite image data : Landsat TM image data was obtained from EOSAT (Earth Observation Satellite Company) for the classification of land surface type, and for the estimation of ground surface temperature. The classification method applied here is Maximum-Likelihood Method.

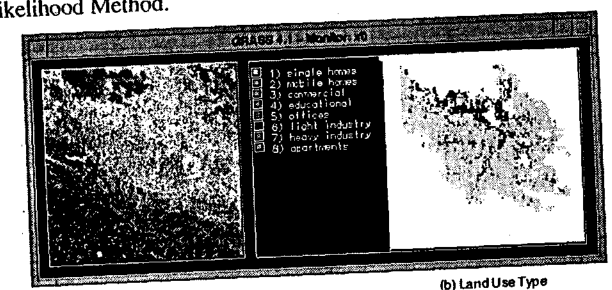

Fig.5 A model city (San Jose Area)

These data, in different spatial resolutions, were converted to raster data of 150 meter cell size by resampling or by blocking operations. The raster data covers 38.4 km by 38.4 km of San Jose area (**Fig.5 (a)-(b)**) which is subdivided into 256 by 256 cells.

Simulation Method

(1) Procedure

Fig.6 illustrates the procedure of the simulation in this case study. The final output is quantitative effects, that is the air temperature drop by the mitigation plans described above. First, using San Jose historical data in GRASS, the contributions of the heat transfer phenomena are calculated with the physical submodels. Then, the contribution of convection and reradiation (ΔT_{inter}) is estimated. In the second step, a neural network is trained with selected data patterns including the estimated ΔT_{inter} and its influential factors.

In the final step, the physical submodels and the cellular automaton submodels with the acquired transition rules are executed under the condition of each mitigation plan. For the cellular automaton submodel, Geocellular (Takeyama, 1993), a graphical interface tool for cellular automaton developed at NCGIA at Santa Barbara was utilized. This tool allows users to execute a cellular automaton language "cellang" (Eckart, 1992) in the Motif window environment.

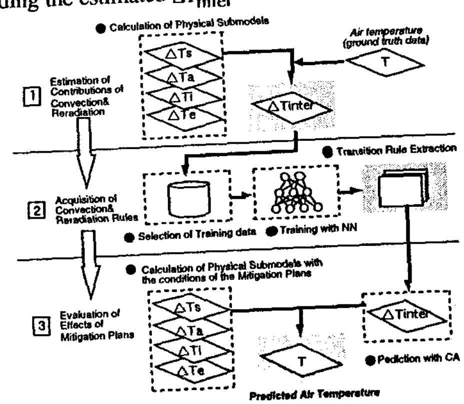

Fig.6 A procedure of the simulation

(2) Transition Rule Extraction

Of the influential factors on the contribution of the convection and reradiation (ΔT_{inter}), four factors were selected based on a priori knowledge and preliminary analysis.

1) wind velocity & direction
2) characteristic of the buildings structure (SVF; Sky View Factor, Oke, 1981),
3) sum of the air temperature differences between eight neighboring cells,
4) contribution by evapotranspiration ΔT_e

Since the cellular automaton basically deals with only integer values, these data were categorized as shown in **Table 1**. **Fig.7** shows the structure of the neural network. A change of ΔT_{inter} in one simulation time step is assign in the output layer of the neural network. In the input layer, four parameters (WI, BU, TD and TE) are assigned as the input neurons. The number of the hidden neuron was determined by the results of several preliminary simulations. The number determined here is 80. As the training data, one hundred transition patterns were selected from the time series historical data in GRASS.

Table 1 Example of category

DT: Change of ΔTinter (dΔTinter)
■ dΔTinter(t) = ΔTinter(t+1) - ΔTinter(t)

category	range (℃)	category	range (℃)
-10	dΔTinter<-9	1	0≤dΔTinter<1
-9	-9≤dΔTinter<-8	2	1≤dΔTinter<2
-8	-8≤dΔTinter<-7	3	2≤dΔTinter<3
-7	-7≤dΔTinter<-6	4	3≤dΔTinter<4
-6	-6≤dΔTinter<-5	5	4≤dΔTinter<5
-5	-5≤dΔTinter<-4	6	5≤dΔTinter<6
-4	-4≤dΔTinter<-3	7	6≤dΔTinter<7
-3	-3≤dΔTinter<-2	8	7≤dΔTinter<8
-2	-2≤dΔTinter<-1	9	8≤dΔTinter<9
-1	-1≤dΔTinter< 0	10	9≤dΔTinter

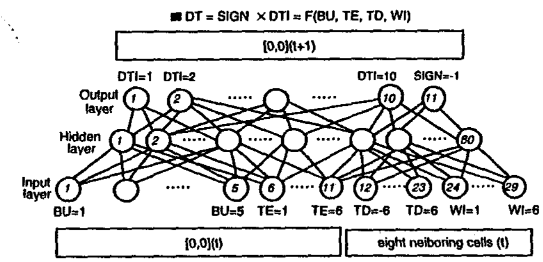

Fig. 7 A structure of the neural network

RESULTS AND DISCUSSIONS

Contributions of the Heat Transfer Phenomena

Fig.8 (a)-(b) show calculated hourly changes of the contributions in two different conditions, vegetation and residential area (Los Gatos Station; N37:14,W121:58) and asphalt/concrete and commercial area (San Jose Station; N37:21,W121:54) respectively. As a background air temperature T_o, the lowest air temperature of the simulated day (July 30, 1992) was used.

As shown in **Fig.8 (a)**, in vegetated areas, the contributions of the solar radiation, the evapotranspiration and the convection and reradiation were predominantly larger than those by others. Although a peak contribution of the evapotranspiration occurred at noon when the intensity of the insolation became maximum, that of the solar radiation appeared at 4pm. This time delay is considered to be caused by the thermal inertia of the ground surface which mediates between the air and the ground surface. The estimated contribution of the convection & reradiation changed in such a manner as to counterbalance the time delay between the solar radiation and the evapotranspiration.

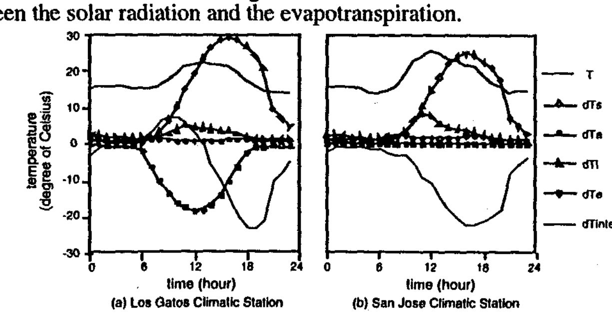

Fig.8 Contribution of the phenomena

In the case of the asphalt/concrete area shown in **Fig.8 (b)**, compared with the vegetation area, the ground surface temperature became relatively higher, and this made the contribution of the infrared radiation larger than that in the vegetation area (e.g. approximately 61% larger at noon). In this case, since there is no contribution of the evapotranspiration, the contribution of the convection and reradiation changed according to the pattern of the solar radiation. In the non-vegetation areas, since the convection is only a major phenomena which functions as a cooling effect during daytime, the urban structure which does not hinder convection is important for the mitigation of the urban heat island.

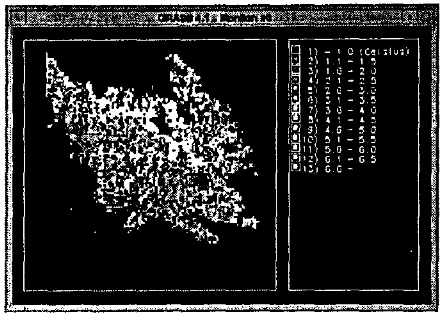

Fig. 9 Distribution of air temperature rise

Table 2 Air temperature rise at 4pm

Building type	Number of cell	average of dTa (degree)
Single family residental	16166	0.93
Mobile home	308	0.91
Commercial	964	2.08
Education	438	1.52
Office	278	2.26
Light industry	1557	1.37
Heavy industry	580	1.45
Apartment	500	1.17

Fig.9 shows the distribution of the contribution by the anthropogenic heat release at 4pm. The degrees of the air temperature rise in non-residential areas were generally larger than in residential areas. As shown in **Table 2**, in office areas, its average was over 2 degrees and its maximum reached up to 7.3 degrees.

Validation of Acquired Transition Rules

The training of the selected transition patterns was iterated until an average of the association error of the output neurons converged (the average of the association error 7.1%). The causal indices (Baba,1990; Embutsu,1991), which represents the degree of the correlation between an input neuron and an output neuron, was calculated with the weight parameters of the network. The input neurons which had larger correlations with the output neurons (DTI, SIGN) were interpreted into if-then type transition rules shown in **Table 3**.

To validate the acquired transition rules, the contribution of the convection and reradiation was predicted with Geocellular using the rules of **Table 3**, and was compared with the true data of ΔT_{inter}. The predicted ΔT_{inter} values on July 30, 1992 at the Los Gatos Climatic Station are shown in **Fig.10**. The predicted values agreed relatively well with the true data. Within a central zone (64 cells by 64 cells) of San Jose, a correlation (r) between the predicted and the true data was 0.71. Although the prediction performance of the acquired transition rules still needs to be further improved, this result shows that some part of the underlying dynamics can be acquired with the proposed method.

Table 3 Acquired transition rules

1	if (TE ≤2 AND TD≤-1) then SIGN=-1
2	if WI ≥3 then SIGN=-1
3	if (TE=1 AND (TD=-1 OR TD=1)) OR WI=1 OR WI=3 OR WI=4 then DTI=1
4	if ((TE=2 OR TE=3) AND TD=1) OR WI=2 then DTI=2
5	if TE=3 AND (TD=2 OR TD=-2) AND WI=2 then DTI=3
6	if TE=3 AND (TD=2 OR TD=-2) AND WI=5 then DTI=4
7	if (TE=4 AND TD≠3) OR WI=6 then DTI=5
8	if TE=4 AND TD=3 then DTI=6
9	if TE≠4 AND TD=3 AND WI=6 then DTI=7
10	if TE=5 AND TD=-3 then DTI=8
11	if TE=5 AND (TD=4 OR TD=-4) then DTI=9
12	if TE=6 AND (TD=4 OR TD=-4) then DTI=10

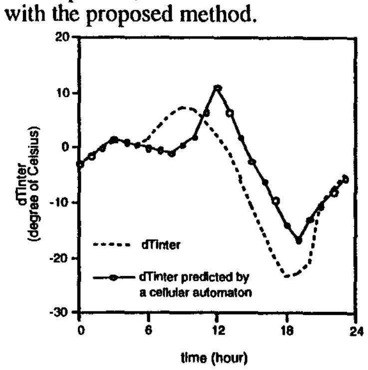

Fig.10 Predicted ΔT_{inter}

Effects of Mitigation Plans

(1) Plan1 : Recovering the waste heat from buildings

In this simulation, the light and the heavy industrial areas (see **Fig.5 (b)**) were assigned as the heat sources to be recovered. The amount of actually recovered heat was determined to be equal to that of heat used as hot water (20% of the total building energy consumption) which did not contribute to the air temperature after using it.

The average of the effects in the light and the heavy industrial areas were 0.20 degrees and 0.22 degrees respectively. These air temperature fall effects were not large enough to spread to neighboring landuse type areas. Since the large heat sources like a power plant and an incinerator do not exist in the industrial area of San Jose, a significant effect could not be proved.

(2) Plan2 : Reducing the waste heat from buildings

In this simulation, the wasted heat from the air conditioner units (in the case of San Jose area, 13% of the total building energy consumption) was assumed to be eliminated. **Table 4** show the air temperature fall at 4pm. The average effects were as small as those by plan1, however, in a built-up area within the commercial and the office areas, the maximum air temperature fall came up to 0.85 degrees, which is regarded sufficient to improve urban comfort.

Since the urban characteristics relevant to this simulation (e.g. energy consumption, etc.) are generally different with each city, the degree of the effects in the San Jose area can not be expected in other cities. However, in larger cities like the Tokyo Metropolitan area, it could be supposed that larger effects would be achieved by this plan, because it has larger building energy consumption (0.32 $MJm^{-2}hr$, floor area basis; Narita,1990).

(3) Plan3 : Reducing the waste heat from automobiles

It was assumed that 30% of traffic flow could be reduced in the commercial, the office and the industrial areas. Regarding the estimation of the traffic heat, it was based on the actual vehicle mileage traveled (City of San Jose, 1993), and the exhausted heat during the idling state (e.g. signal stop) was not included due to a lack of data.

Fig.11 shows the air temperature fall by this plan at 4pm, when the evening traffic congestion starts. Larger air temperature fall than previous two plans was achieved in every area. As shown in **Table 4**, the degree of the effects was approximately twice as large as those by plan 2. It can be said that this mitigation plan is most effective if this level of the traffic flow reduction could be realized.

Table 4 Effects of mitigation plans

Building type	Number of cell	Effect (degree)		
		Plan1	Plan2	Plan3
Single residental	16166	-	0.08	0.14
Mobile home	308	-	0.08	0.15
Commercial	964	-	0.19	0.60
Education	438	-	0.14	0.14
Office	278	-	0.22	0.64
Light industry	1557	0.20	0.12	0.44
Heavy industry	580	0.22	0.14	0.47
Apartment	500	-	0.11	0.16

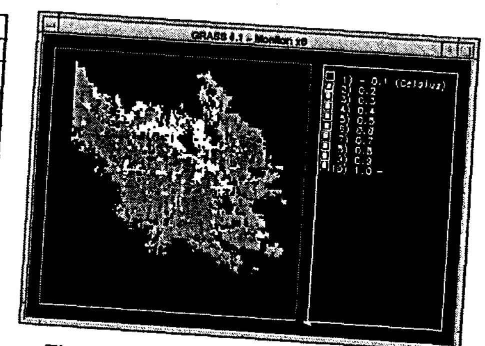

Fig. 11 Effect of mitigation plan3 at 4pm

CONCLUSIONS

This study showed that the urban heat island can be mitigated to some extent by the proposed plan featuring the DHC plant or the traffic control. The accomplishment of the proposed mitigation plans still needs to be investigated from other viewpoints, because allocating the DHC plants and the traffic control are naturally related to many urban activities which have a higher priority than the urban heat island problem for the urban residents. A further analysis with the GIS linked to models of other urban activities will be able to show the impact of the mitigation plans on other urban activities, and by this, the plans will be expected to be made more feasible and concrete.

Acknowledgements

This research was supported by the National Center for Geographic Information and Analysis (NCGIA) at Santa Barbara and Hitachi America, Ltd. The authors would like to thank Mr. Ken'ichiro Oka (Hitachi, Ltd.), Mr. Paul Sorensen and Mr. Thomas Cova (University of California at Santa Barbara) for their help and useful discussions.

Reference

Baba, K. et al. (1990) Explicit Representation of Knowledge Acquired from Plant Historical Data Using Neural Network, *Proceedings of IJCNN-San Diego*

City of San Jose, California (1993) *Environmental Scan of the city of San Jose*

Doorenbos, J. (1977) Guidelines for Predicting Crop Water Requirements, *FAO irrigation and drainage paper 24*, FAO of the United Nations

Eckart, J. (1992) *A Cellular Automata Simulation System : Version 3.0*, Department of Computer Science, Radford University

Embutsu, I. et al. (1991) Fuzzy Rule Extraction from a Multilayered Neural Network, *Proceedings of IJCNN-Seattle*

Goodchild, M. et al. (1993) *Environmental Modeling with GIS*, Oxford University Press

Khan, A. (1993) *Energy Efficiency and Environmental Quality Through Intelligent Vehicle Highway Systems (IVHS) Technologies*, Proceedings of IEE Vehicle Navigation & Information Systems Conference '93, IEEE

Kraushaar, J. et al. (1993) *Energy and Problems of a Technical Society - Second Edition*, John Wiley & Sons, Inc.

Landsberg, H. (1981) *The Urban Climate - International Geophysics Series Vol.28*, Academic Press

Mall, G. (1989) Cooling Our Baking Cities, *American Forests*, **95**

Narita, K. et al. (1990) Energy Recycling System for Urban Waste Heat, *Energy and Buildings*, **15**

Oke, T. (1976) The Distinction Between Canopy and Boundary Layer Urban Heat Islands, *Atmosphere*, **14**

Oke, T. (1978) *Boundary Layer Climates*, Methuen & Co.,Ltd.

Oke, T. (1981) Canyon Geometry and the Nocturnal Urban Heat Island - Comparison of Scale Model and Field Observations, *Journal of Climatology*, **1**

Ojima, T. (1990) Changing Tokyo Metropolitan Area and its Heat Island Model, *Energy and Buildings*, **16**

Pacific Gas & Electric Company (1992) *Final Report - Conditional Demand Analysis*

Rumelhart, D. (1986) Learning Internal Representations by Error Propagation, *Parallel Distributed Processing Vol.1*, MIT Press

Saito, T. (1992) *Global Warming and Urban Heat Islands* (Japanese), Morikita Syuppann

Shapiro, M. et al. (1993) *GRASS4.1 Programmer's Manual*, U.S. Army Construction Engineering Research Laboratory

Sharin, N. (1984) The Urban Complex as a Factor in the Air-temperature pattern in a Mediterranean Coastal Region, *Energy and Buildings*, **7**

Simonett, D. et al. (1988) Estimation of the Magnitude and Spatial Distribution of Combustible Materials in Urban Areas - A case study of the San Jose area, California, *Fire and Materials*, **12**

Swaid, H. (1990) Prediction of Urban Air Temperature Variations Using the Analytical CTTC Model, *Energy and Buildings*, **14**

Takeyama, M. (1993) *Geocellular*, Technical Report, National Center for Geographic Information & Analysis, University of California at Santa Barbara

Terjung, W. (1980) Simulating the Causal Elements of the Urban Heat Island, *Boundary Layer Meteorology*, **19**

U.S. Department of Energy (1992) *Annual Energy Review 1991*, DOE/EIA-0384(91)

MAPPING FOREST DISTRIBUTIONS OF CENTRAL AMERICA AND MEXICO

Susan Eggen-McIntosh, Keith B. Lannom, and Dennis M. Jacobs
USDA Forest Service
Southern Forest Experiment Station
Forest Inventory and Analysis (SO-FIA)
P.O. Box 906
Starkville, MS 39759 USA

ABSTRACT

Central America and Mexico have the second highest deforestation rate of global tropical country groups (FAO 1993). Where are the remaining forests and what type are they? No regional maps are currently available. Methods developed for mapping forest distributions of the United States (Zhu 1994) are being applied to Mexico and Central America to provide a synoptic, current view of forest distributions using a consistent methodology. A cooperative effort with forestry agencies of Mexico and Central America, United States governmental agencies, and non-governmental agencies is described here. Forest cover of 15 Landsat* Thematic Mapper (TM) or Système Probatoire d'Observation de la Terre (SPOT) images are being classified and verified using existing maps, historical aerial photography, and airborne videography with global positioning system (GPS) coordinates (Eggen-McIntosh *et al.* [in press]) input to a geographic information system (GIS). Percent forest cover will be modeled with weather satellite image cloud-free composite bands as the independent variables. Areas identified as forest will then be classified using the weather satellite composites and GIS coverage of rainfall and elevation data. Results will be GIS coverages of percent forest cover and forest type distributions for resource analyses.

BACKGROUND

The United Nations' Food and Agricultural Organization (FAO) Forest Resource Assessment (FRA) 1990 Project estimated that the two highest rates of worldwide tropical deforestation occur in continental southeast Asia (1.6%) and Central America and Mexico (1.5%). These annual deforestation rates are more than twice those of tropical South America and of Africa, both with 0.7% (FAO 1993). The FRA aggregated sub-national estimates of forest area and volume to report national statistics, but did not report within-country distributions. How are the remaining forests of Central America and Mexico distributed?

---

*Mention of company or product names is for information only and does not constitute official endorsement by the USDA Forest Service.